JACS
JOURNAL OF THE AMERICAN CHEMICAL SOCIETY

Article

pubs.acs.org/JACS

A Paramagnetic Heterobimetallic Polymer: Synthesis, Reactivity, and Ring-Opening Polymerization of Tin-Bridged Homo- and Heteroleptic Vanadoarenophanes

Holger Braunschweig,*[,†] Alexander Damme,[†] Serhiy Demeshko,[‡] Klaus Dück,[†] Thomas Kramer,[†] Ivo Krummenacher,[†] Franc Meyer,[‡] Krzysztof Radacki,[†] Sascha Stellwag-Konertz,[†] and George R. Whittell[§]

[†]Institut für Anorganische Chemie, Julius-Maximilians-Universität Würzburg, Am Hubland, 97074 Würzburg, Germany

[‡]Institut für Anorganische Chemie, Georg-August-Universität Göttingen, Tammannstrasse 4, 37077 Göttingen, Germany

[§]School of Chemistry, University of Bristol, Cantocks Close, Bristol BS8 1TS, United Kingdom

Supporting Information

ABSTRACT: The synthesis of the first tin-bridged bis(benzene) vanadium and trovacene sandwich compounds and the investigation of their oxidative addition and insertion behavior are reported. The vanadoarenophanes and the corresponding platinum insertion products were fully characterized including electrochemical and electron paramagnetic resonance (EPR) measurements. Controllable ring-opening polymerization of the heteroleptic tin-bridged [1]-trovacenophane using Karstedt's catalyst yields a high molecular weight polymer (up to M_n = 89 200 g·mol^{-1}) composed of d^5-vanadium metal centers in the main chain, making it a rare example of a spin-carrying macromolecule. Magnetic susceptibility measurements (SQUID) confirm the paramagnetic scaffold with repeating S = 1/2 centers in the main chain and suggest antiferromagnetic interactions between adjacent spin sites (Weiss constant Θ = −2.9 K).

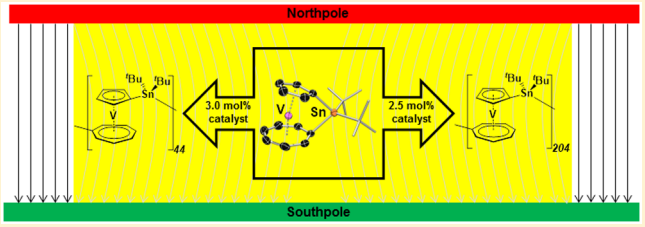

INTRODUCTION

Since the first report of high molecular weight polymers based on ferrocene by Withers and Seyferth[1] and Brandt and Rauchfuss,[2] the preparation of poly(metallocenes) has received growing interest. There have been various synthetic approaches to poly(ferrocenes), including the condensation of unstrained dihaloboryl derivatives with triethylsilane to give borylene-bridged macromolecules.[3] In 1992, Manners' group achieved a breakthrough in this respect with the so-called ring-opening polymerization (ROP) of strained *ansa* ferrocene precursors.[4] During the following years several variants of this method were developed including anionic, photoinduced, thermal, or transition-metal-mediated polymerization.[5] Most of these ROP reactions rely on the use of single-atom bridged *ansa* ferrocenes, in which the nature of the bridging moiety can vary from group 13 (B, Al, In, Ga)[6] to group 14 (Si, Ge, Sn),[7] group 15 (P, As),[1,7a,8] and group 16 elements (S, Se).[9] Although main-group elements represent the majority of bridging units, it has also been possible to incorporate early and late transition metals of group 4 (Ti, Zr, Hf)[10] and group 10 (Ni, Pt)[11] into the ligand-sphere of metallocenes. Moreover, several paramagnetic bridged and unbridged 17-electron ferrocenium species are known.[12]

While ferrocene plays a prevalent role in this field because of its ease of preparation and well-established dilithiation protocol,[13] other sandwich compounds have also been the subject of investigations. Recently, several diamagnetic metalloarenophanes derived from [M(η^6-C$_6$H$_6$)$_2$] (M = Cr, Mo)[14] and [M(η^5-C$_5$H$_5$)(η^7-C$_7$H$_7$)] (M = Ti, Cr)[15] have been prepared and, in some instances, successfully polymerized by ROP.[15d,16] Some systems, like the sandwich compounds of titanium,[17] chromium,[18] or rhodium,[19] show the potential to access different oxidation states. Furthermore, cationic *ansa*-derivatives are known, for example, of cobaltocene[12e,20] or [Ti(η^5-C$_5$H$_5$)(η^8-C$_8$H$_8$)].[21]

Despite numerous examples of paramagnetic, strained *ansa* compounds, their electrochemical and polymerization behavior has only been scarcely studied so far.[22] In particular, bridged complexes of bis(benzene) vanadium [V(η^6-C$_6$H$_6$)$_2$][14g,23] and the corresponding isoelectronic mixed sandwich complex [V(η^5-C$_5$H$_5$)(η^7-C$_7$H$_7$)] (also known as trovacene)[24] have long been a subject of great interest. Nevertheless, the first polymer derived thereof was only obtained in 2008 by Pt-catalyzed ROP of [V(η^6-C$_6$H$_5$)$_2$SiMe^{i}Pr] (**1**),[25] yielding polymers with silicon in the main chain (Scheme 1).[24c]

Because of the high density of unpaired spins, these polymers are expected to exhibit remarkable physical properties with

Received: October 23, 2014
Published: January 5, 2015

DOI: 10.1021/ja510884h
J. Am. Chem. Soc. 2015, 137, 1492−1500

Scheme 1. Transition Metal-Catalyzed Polymerization of Paramagnetic Vanadium Sandwich Compounds

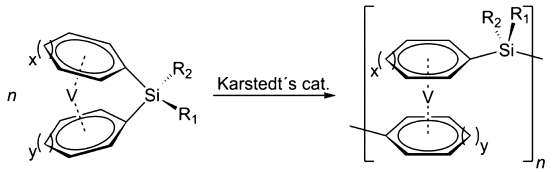

1: x = 1, y = 1; R_1 = Me, R_2 = ^{i}Pr
2a: x = 0, y = 2, R_1 = R_2 = Me
2b: x = 0, y = 2, R_1 = Me, R_2 = ^{i}Pr

3: x = 1, y = 1; R_1 = Me, R_2 = ^{i}Pr
4a: x = 0, y = 2, R_1 = R_2 = Me
4b: x = 0, y = 2, R_1 = Me, R_2 = ^{i}Pr

regard to magnetism or conductivity. Elschenbroich et al. showed that silicon-bridged dimers of bis(benzene) vanadium[26] as well as di- and tetranuclear trovacenyl units with tin as spacer show a pronounced intramolecular electronic and magnetic communication.[27]

In this context, the synthesis of new, strained tin-bridged paramagnetic *ansa* sandwich compounds became a major focus of our studies. While several metallocenes and metalloarenes with tin in the bridging unit were successfully synthesized,[7c,d] the preparation of derivatives with a single-atom linker remains challenging.[15e,28] It is important to note that the bond between the *ipso*-carbon and tin is rather weak, so that bulky substituents are required to allow their isolation and avoid spontaneous ring-opening reactions.[15e] In spite of having a lower tilt angle α in comparison to their lighter analogues, the ease of bond cleavage makes these molecules excellent precursors for ROP (see Table 1 for a definition of the tilt angle α).[7d]

Herein, we report the synthesis and properties of strained, tin-bridged [1]vanadoarenophanes, which have been fully characterized by electron ionization mass spectrometry (EI-MS), X-ray diffraction, UV−vis, and EPR spectroscopy. Furthermore, we present reactivity studies toward $[Pt(PEt_3)_3]$ and the formation of a paramagnetic polymer derived from a tin-bridged trovacene.

RESULTS AND DISCUSSION

Synthesis and Characterization of $[V(\eta^6\text{-}C_6H_5)_2Sn^tBu_2]$ (5) and $[V(\eta^5\text{-}C_5H_4)(\eta^7\text{-}C_7H_6)Sn^tBu_2]$ (6). The tin-bridged vanadoarenophanes were prepared by salt elimination reactions between the respective dilithiated sandwich compounds and di-*tert*-butyltin dichloride at −78 °C (Scheme 2). During the course of the reaction, the color changed from brown to red in the case of **5** and from gray to purple in the case of compound **6**. After workup and recrystallization from pentane at −70 °C, the products were obtained as crystalline solids in moderate yields (**5**, 29%; **6**, 38%). The complexes were characterized by elemental analysis and mass spectrometry. In both cases, the molecular ion peaks at m/z = 439 clearly confirm the expected composition of **5** and **6**. Crystals suitable for solid-state characterization by X-ray diffraction could be obtained by recrystallization from pentane at −30 °C (Figure 1). While compound **5** crystallizes in the monoclinic space group *C2/c*, compound **6** crystallizes in the monoclinic space group $P2_1/c$.

Scheme 2. Synthesis of the [1]Stannavanadoarenophanes 5 and 6

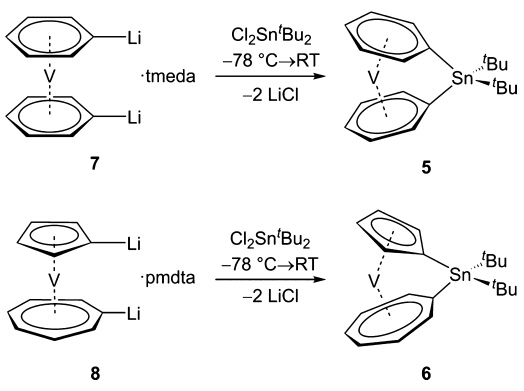

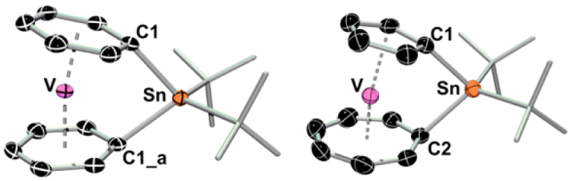

Figure 1. Molecular structures of $[V(\eta^6\text{-}C_6H_5)_2Sn^tBu_2]$ (**5**, left) and $[V(\eta^5\text{-}C_5H_4)(\eta^7\text{-}C_7H_6)Sn^tBu_2]$ (**6**, right). Hydrogen atoms and ellipsoids of the substituents on the tin atom are omitted for clarity. Symmetry-related positions (**5**: $-x + 1, y, -z + 3/2$) are labeled with _a. Thermal ellipsoids are displayed at the 80% (**5**) and 50% (**6**) probability level. Selected bond lengths [pm] and angles [deg]: **5**, V−X_{Bz} 168.7, C1−Sn−C1_a 85.4(1), α = 15.6(1), β = 34.9, δ = 168.0; **6**, V−X_{Cp} 213.0, V−X_{Cht} 150.1, C1−Sn−C2 87.1(2), α = 12.8(2), β_{Cp} = 29.5, β_{Cht} = 44.8, δ = 170.1 (X_{Bz} = centroid of the C_6H_5 ring, X_{Cp} = centroid of the C_5H_4 ring, X_{Cht} = centroid of the C_7H_6 ring).

Table 1. Structural Parameters of [1]- and [2]Bis(benzene) Vanadoarenophanes (Bz = C_6H_5 Ring)

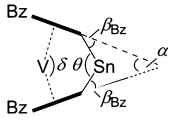

	5	9[26b]	11
α [°]	15.6(1)	19.9	7.5(5)
β_{Bz} [°]	34.9	23	Sn, 15.1; Pt, 9.7
δ [°]	168.0		173.6

The insertion of a single-atom tin bridge distorts the carbocyclic ring planes from a parallel arrangement (**5**, V−C_{Bz} 217.7(2)−224.3(2) pm; **6**, V−C_{Cp} 222.8(3)−228.3(3) pm, V−C_{Cht} 215.7(3)−220.1(3) pm), resulting in moderate deformation angles of δ = 168.0° (**5**) and δ = 170.1° (**6**) (see Tables 1 and 2). As expected, the tilt angles of **5** (α = 15.6(1)°) and **6** (α = 12.8(2)°) differ slightly because of the larger interannular

Table 2. Structural Parameters of [1]- and [2]Trovacenophanes (Cp = C_5H_4 Ring; Cht = C_7H_6 Ring)

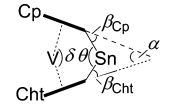

	2b[24c]	6	10[24c]	12
α [°]	18.3(2)	12.8(2)	17.7(2)	6.7(2)
β_{Cp} [°]	31.8	29.5	29.3	7.5
β_{Cht} [°]	46.4	44.8	45.2	1.5
δ [°]	166.1	170.1	166.1	175.1

DOI: 10.1021/ja510884h
J. Am. Chem. Soc. 2015, 137, 1492−1500

distance in trovacene in comparison with bis(benzene) vanadium. Furthermore, the C_{ipso}–Sn bonds are considerably twisted out of the ring planes (**5**, β = 34.9°; **6**, β_{Cp} = 29.5, β_{Cht} = 44.8), and the C_{ipso}–Sn–C_{ipso} angles deviate significantly from an ideal tetrahedral angle (**5**, θ = 85.4(1)°; **6**, θ = 87.1(2)°). Because of the higher covalent radius of Sn compared to its lighter congeners, the [1]stannavanadoarenophanes exhibit less molecular strain than the corresponding silicon or germanium compounds ([V(η^6-C_6H_5)$_2$Si(C_3H_6)] (**9**), α = 19.9°;[26b] [V(η^5-C_5H_4)(η^7-C_7H_6)SiMe^{i}Pr] (**2b**), α = 18.3(2)°; [V(η^5-C_5H_4)(η^7-C_7H_6)GeMe$_2$] (**10**), α = 17.7(2)°).[24c]

In addition, we investigated the fate of compound **5** upon air exposure (Scheme 3). Related *ansa* complexes like [V(η^6-C_6H_5)$_2$BN^{i}Pr$_2$] or [V(η^6-C_6H_5)$_2$Si$_2$Me$_4$] show decomposition to a vanadium-containing precipitate and the free ligand system.[23c] Likewise, controlled decomposition of **5** leads to an insoluble solid of unknown composition and the free ligand, as judged by ^{1}H NMR spectroscopy (δ = 1.32 ppm (s, 18 H, Sn^{t}Bu$_2$), 7.14–7.64 ppm (several m, 10 H, phenyl groups)). On the other hand, the trovacene compound **6** did not show any signs of controlled decomposition upon air exposure.

Scheme 3. Decomposition Pathway of [V(η^6-C_6H_5)$_2$Sn^{t}Bu$_2$] (5) upon Air Exposure

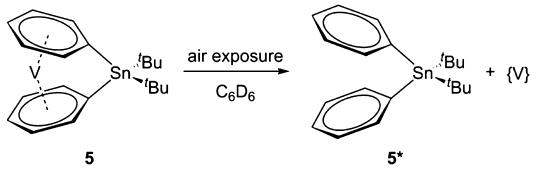

Reactivity of 5 and 6 toward [Pt(PEt$_3$)$_3$]. As our initial attempts to initiate an anionic polymerization[29] of compounds **5** and **6** failed and, in addition, no hints for a thermal ROP could be observed in differential scanning calorimetry (DSC) measurements (see Figures S1 and S2, Supporting Information),[7d] the compounds were studied with regard to the activation of the C_{ipso}–Sn bond by transition metal compounds. Previous work has shown that [1]stannaferrocenophanes and other tin-bridged sandwich compounds undergo carbon-element bond activation by various Pt complexes.[7d,15e,28]

To this end, compound **5** and **6** were treated with an equimolar amount of [Pt(PEt$_3$)$_3$] in toluene and heated to 60 °C over a period of 24 h (Scheme 4). The reaction resulted in the isolation of platina-di-*tert*-butylstanna[2]bis(benzene)-vanadoarenophane (**11**) as red-brown and platina-di-*tert*-butylstanna[2]trovacenophane (**12**) as gray powder in moderate yields (**11**, 47%; **12**, 39%; Scheme 4).

Scheme 4. Oxidative Addition of the C_{ipso}–Sn Bond in 5 and 6 to [Pt(PEt$_3$)$_3$]

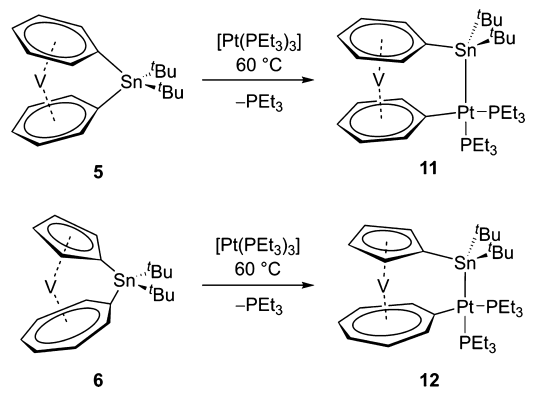

The insertion products were characterized by elemental analysis and X-ray diffraction. Suitable crystals for X-ray structural analysis were obtained by slow crystallization from tetrahydrofuran (THF) solutions at −30 °C (see Figure 2). In

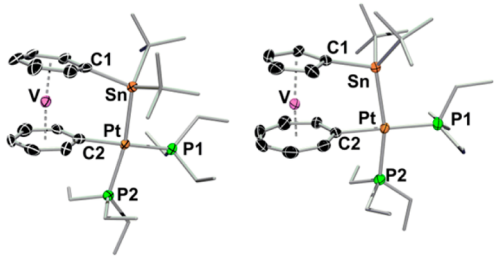

Figure 2. Molecular structures of [V(η^6-C_6H_5)$_2$Sn(^{t}Bu$_2$)Pt(PEt$_3$)$_2$)] (**11**, left) and [V(η^5-C_5H_4)(η^7-C_7H_6)Sn(^{t}Bu$_2$)Pt(PEt$_3$)$_2$] (**12**, right). Hydrogen atoms and ellipsoids of the substituents on the tin and phosphorus atoms are omitted for clarity. Thermal ellipsoids are displayed at the 80% (**11**) and 50% (**12**) probability levels. Selected bond lengths [pm] and angles [deg]: **11**, V–X_{Bz} 163.9 and 166.6, Pt–P1 229.6(2), Pt–P2 237.1(2), C1–Sn–Pt 108.9(2), C2–Pt–Sn 82.9(2), C2–Pt–P1 173.8(2)°, α = 7.5(5), β_{Cp} = 15.1, β_{Cht} = 9.7, δ = 173.6; **12**, V–X_{Cp} 188.3, V–X_{Cht} 144.8, Pt–P1 229.3(1), Pt–P2 234.6(1), C1–Sn–Pt 108.8(1), C2–Pt–Sn 84.8(1), C2–Pt–P1 179.1(2)°, α = 6.7(2), β_{Cp} = 7.5, β_{Cht} = 1.5, δ = 175.1 (X_{Bz} = centroid of the C_6H_5 ring, X_{Cp} = centroid of the C_5H_4 ring, X_{Cht} = centroid of the C_7H_6 ring).

comparison to the single-atom bridged complexes, the oxidative addition of a Pt^0 fragment decreases the tilt angle and increases the deformation angle (**11**, α = 7.5(5)°, δ = 173.6°; **12**, α = 6.7(2)°, δ = 175.1°), consistent with a reduction of ring strain. The lighter analogues [V(η^6-C_6H_5)$_2$SiMe^{i}Pr][25] and [V(η^5-C_5H_4)(η^7-C_7H_6)SiMe$_2$] (α = 10.6°, δ = 171.9°)[30] react in a similar manner, whereas the products of the oxidative addition of the silicon-bridged bis(benzene) vanadium compounds have never been structurally characterized to the best of our knowledge. Furthermore, the insertion products show the expected square-planar environment at the Pt moiety (**11**, C2–Pt–Sn 82.9°, C2–Pt–P1 173.8(2)°; **12**, C2–Pt–Sn 84.3(2)°, C2–Pt–P1 179.1(2)°) with Pt–P1 bonds that are slightly shorter than those between Pt and P2 (**11**, Pt–P1 229.6(2) pm, Pt–P2 237.1(2) pm; **12**, Pt–P1 229.3(1) pm, Pt–P2 234.6(1) pm), as a result of the trans influence of the organotin fragment. Moreover, we note a regioselective bond cleavage of the C_{ipso}–Sn bond between the cycloheptatrienyl ring and the bridging element in compound **12**, as was previously observed in other systems ([V(η^5-C_5H_4)(η^7-C_7H_6)SiMe$_2$][30] and [Ti(η^5-C_5H_4)(η^5-C_7H_6)Sn^{t}Bu$_2$]).[15e] The observed regioselectivity is consistent with the rationale that the C_{ipso}–Sn bond associated with the higher β angle is more susceptible to bond cleavage.

ROP Studies. With these results in hand and the knowledge that Karstedt's catalyst, Pt$_2$[(CH$_2$CHSiMe$_2$)$_2$O]$_3$, successfully initiates the polymerization of similar systems,[24c,25] we attempted to polymerize the [1]stannavanadoarenophanes **5** and **6**. Thus, toluene solutions of each compound were combined with Karstedt's catalyst (1–3.0 mol%) and then heated at 60 °C for ∼12 h. Subsequently, the resulting mixtures were precipitated into hexane to purify the polymeric material from short-chain oligomers. In the case of **5**, all attempts to

DOI: 10.1021/ja510884h
J. Am. Chem. Soc. 2015, 137, 1492–1500

produce polymeric structures by varying the mol% of the catalyst resulted in either decomposition of the monomer or isolation of the starting material. However, the addition of 2.5 mol% and 3.0 mol% Karstedt's catalyst to a toluene solution of **6** resulted in an immediate color change from light purple to dark green and gave a light purple solid in 46% yield (**13a**, 3.0 mol%) and a deep purple solid in 44% yield (**13b**, 2.5 mol%) after precipitation into hexane (Scheme 5).

Scheme 5. Polymerization of 6 Using Karstedt's Catalyst

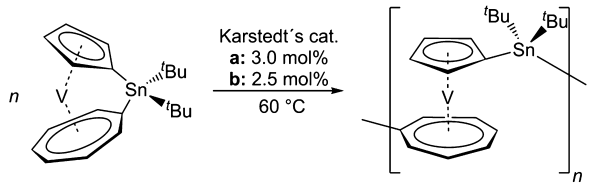

6 **13a** $n \approx 44$ **13b** $n \approx 99/204$

To assess the polymeric nature of **13a** and **13b**, the molecular weight was determined by gel permeation chromatography (GPC) in THF, relative to a series of monodisperse polystyrene standards. In case of **13a**, the number-average molecular weight (M_n) was determined to be 19 300 g·mol^{-1} with a polydispersity index (PDI = M_w/M_n) of 1.82 (see Figure S3 in Supporting Information). This value corresponds to a number-average degree of polymerization (DP_n) of 44 (m = 438.09 g·mol^{-1}). Using just 2.5 mol% of the catalyst, a polymer with a higher M_n of 43 200 g·mol^{-1} (DP_n = 99) and PDI of 2.40 could be isolated (Figure S4, Supporting Information). The chromatograms for **13a** and **13b**, however, exhibited significant tailing to lower molecular weight, which suggested that interactions with the GPC columns were complicating the size-exclusion process. To investigate these phenomena further and their effect on the GPC-determined molecular weights, compound **13b** was reanalyzed using THF that contained 0.1 w/w% [n-Bu$_4$N]Br and toluene (1% v/v) as the flow rate marker. Under these conditions, a M_n of 89 200 g·mol^{-1} (DP_n = 204) and PDI 1.82 were obtained, along with a more Gaussian peak shape (see Figure S5, Supporting Information). The determination of a larger molecular weight in this instance is consistent with a reduction in polar column–coil interactions, as a result of charge screening by the additive. This finding suggests that the values obtained with pure THF should be viewed as underestimates of the true values. While it is stable under an inert atmosphere, exposure to air leads to decomposition of the polymeric structure within 1h, as indicated by a distinct color change from purple to brown.[24c] It was therefore important to confirm that the material eluted unchanged from the GPC column, as this technique cannot be performed with the rigorous exclusion of air. Dynamic light scattering (DLS) was conducted on **13b** as a THF solution, prepared with the exclusion of both air and moisture. This technique revealed a bimodal distribution of hydrodynamic radii (R_h) of 3.8 and 14.5 nm, which represented 62.8 and 37.2% of the scattering volume, respectively (Figure S6, Supporting Information). Relative to monodisperse polystyrene samples in solution, these sizes correspond to molecular weights of 20 700 and 225 400 g·mol^{-1}.[31] The former is less than that observed by GPC under comparable conditions (M_n = 43 200 g·mol^{-1}) but confirms that high polymer is present prior to interactions with the GPC columns and air. This discrepancy most probably results from differences in polydispersity and limitations with the Stokes–Einstein model. The larger population by size would appear to arise from aggregation of the polymer coils at the concentration investigated (2 mg·mL^{-1}), as there is no corresponding peak in the GPC chromatogram. This would suggest that THF is a thermodynamically marginal solvent for **13a** and **13b**. For comparison, the polymerization of the silicon-bridged species **2a** and **2b** under comparable conditions produces polymers with a significantly lower number-average degree of polymerization of 38 (**2a**: M_n = 10 000 g·mol^{-1}, PDI = 2.31, R_h = 3.4 nm) and 20 (**2b**: M_n = 5 600 g·mol^{-1}, PDI = 1.64, R_h = 2.3 nm), respectively.[24c]

EPR Spectroscopy. Fluid solution continuous-wave (CW) EPR spectra of all compounds were recorded at X-band, the results of which are summarized in Table 3. The EPR spectra of

Table 3. Summary of EPR Spectroscopic Parameters for the Different [n]Vanadoarenophanes

	a_{iso}(^{51}V) [G]	g_{iso}
5	57.8	1.987
6	68.5	1.984
11	62.3	1.993
12	71.1	1.988
13a		1.974
13b	*a*	*a*

[a]No signal found.

the monomeric *ansa* complexes **5** and **6** as well as the platinum inserted species **11** and **12** display eight hyperfine lines (I = 7/2 for ^{51}V) that vary in their line widths and spacings as a result of g and a anisotropies that are not completely averaged out in solution (see Figure 3 and Figure S7, Supporting Information). Taking the tumbling of the molecules into consideration (rotational correlation times of 0.1–1 ns in pentane and THF solutions), the EPR spectra can be accurately simulated (see

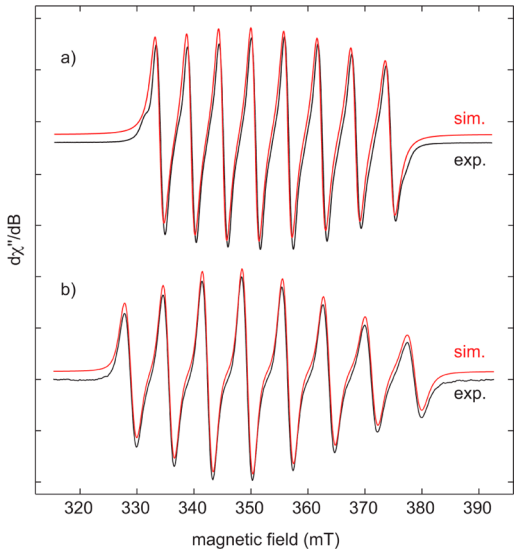

Figure 3. CW EPR spectra of **5** (a) and the corresponding platinum C–Sn insertion complex **11** (b) in pentane (**5**) and THF solution (**11**) at room temperature. The shoulders at the $m_I = \pm 7/2$ transitions seen for compound **5** are likely due to further anisotropic contributions from slow Brownian reorientation.

DOI: 10.1021/ja510884h
J. Am. Chem. Soc. 2015, 137, 1492–1500

also Figure S7, Supporting Information).[32] Detailed studies by Elschenbroich and co-workers have shown that the vanadium hyperfine coupling constant correlates with the tilt angle α in these [*n*]vanadoarenophanes.[14g,24a] By decreasing the tilt angle (less molecular strain), higher hyperfine coupling constants are observed. The same trend is found for the dinuclear transition-metal complexes **11** and **12** in comparison to their mononuclear counterparts **5** and **6**, which is consistent with extension of the *ansa* bridge through Pt insertion into the C−Sn bond.

In contrast, polymer **13a** displays a single broad line (line width = 140 G) with no resolved metal hyperfine splittings (see Figure S8, Supporting Information), thereby precluding the possibility to determine the hydrodynamic radius via the correlation time. The spectral profile, however, is in line with the formation of a ring-opened microstructure including multiple nonequivalent paramagnetic centers and is further consistent with the data of a silicon-containing trovacenyl polymer.[24c] The longer-chain polymer **13b** exhibit no EPR signal down to 20 K, suggesting that the spin-lattice relaxation becomes extremely short due to interactions between the unpaired electrons.

UV−Vis Spectroscopy. The electronic structure of the compounds was probed by solution UV−vis spectroscopy in THF in a range of 220−700 nm. The spectrum of $[V(\eta^6\text{-}C_6H_5)_2Sn^tBu_2]$ (**5**) (see Figure S9, Supporting Information) shows two absorption bands at 325 and 436 nm that are only slightly shifted in comparison to $[V(\eta^6\text{-}C_6H_6)_2]$ (320 and 445 nm).[33] This finding is in line with the known dependence of the UV−vis transition with the tilt angle of the bis(benzene) vanadium complexes, as already observed for $[V(\eta^6\text{-}C_6H_5)_2SiMe^iPr]$ (428 nm) and $[V(\eta^6\text{-}C_6H_5)_2BN^iPr_2]$ (416 nm), which show blue-shifted absorptions with increasing tilt angles.[23c] According to the literature, the high-energy bands can be ascribed to charge transfer as well as intraligand transitions and the low-energy bands represent transitions from the singly occupied molecular orbital (SOMO) into molecular orbitals with ligand, metal, or mixed ligand-metal character. The absorption bands in between can be assigned to metal-to-ligand charge-transfer transitions.[23c,33] Correspondingly, $[V(\eta^6\text{-}C_6H_5)_2Sn(^tBu_2)Pt(PEt_3)_2]$ (**11**) (see Figure S9 in Supporting Information), with a longer bridge and thus a smaller tilt angle, displays red-shifted absorption bands (341 and 462 nm) compared to **5**. In contrast to ferrocene, which shows red-shifted UV−vis bands with increasing tilt angles, *ansa* complexes derived from $[V(\eta^6\text{-}C_6H_6)_2]$ seem to follow an opposite trend (see Table 4 and Figure S9, Supporting Information).[23c] The reason for this different behavior has not yet been established in detail.

Investigation of compound **6** by UV−vis spectroscopy (see Figures S10 and S11, Supporting Information) reveals an absorption band at 213 nm with a shoulder at ca. 320 nm and a weaker band at longer wavelength (611 nm). In contrast to the spectroscopic data of **6**, the platinum-inserted complex **12** (see Figures S10 and S11, Supporting Information) shows two shoulders at ca. 290 and 350 nm together with a strong absorption band at 216 and a weak one at 571 nm. Similarly, polymer **13a** (see Figure S12, Supporting Information) undergoes electronic transitions in the same energy range with two peaks at 269 and 284 nm, two shoulders at ca. 310 and 456 nm, and two maximum absorption wavelengths (460 and 582 nm). Conversely, the longer-chain polymer **13b** (see Figure S13, Supporting Information) shows an absorption band at 258 nm, two ill-defined shoulders at ca. 310 and 370 nm as well as two maximum absorptions at 467 and 602 nm. For comparison, the spectrum of the parent compound $[V(\eta^5\text{-}C_5H_5)(\eta^7\text{-}C_7H_7)]$ shows absorption bands at 243 nm and a shoulder at 274 nm, which can be assigned to intraligand charge-transfer processes.[34] In addition, two ill-defined shoulders at around 300 and 340 nm, resulting from ligand-to-metal and metal-to-ligand charge-transfer transitions, are observed.[34a] Finally, the broad absorption maximum at 571 nm can be attributed to electronic transitions from the SOMO to orbitals with metal- or ligand-character.[34a] It should be noted that this data cannot provide a definite correlation between the observed absorption bands and the existing molecular strain of the compounds (Table 4).

Table 4. Correlation between λ_{max} and the Tilt Angle α

	λ_{max} [nm]	ε [L·mol^{-1}·cm^{-1}]	α [°]
$[V(\eta^6\text{-}C_6H_5)_2BN^iPr_2]$[23c]	416	2753	29.4
$[V(\eta^6\text{-}C_6H_5)_2SiMe^iPr]$[23c]	428	2458	20.9
5	436	2925	15.6
11	462	3157	7.5
$[V(\eta^6\text{-}C_6H_6)_2]$[33]	445	1123	
6	611	64	12.8
12	571	104	6.7
13a	460, 582		
13b	467, 602		
$[V(\eta^5\text{-}C_5H_5)(\eta^7\text{-}C_7H_7)]$[34]	563	33	

Cyclic Voltammetry. The redox behaviors of the parent sandwich compounds (**5** and **6**) and the polymers (**13a**/**b**) were examined by cyclic voltammetry in THF solution (see Figures S14, S15, S18, and S19 in the Supporting Information). While **5** displays an irreversible oxidation wave at $E_{pa} = -0.8$ V, **6** shows an anodically shifted quasi-reversible oxidation wave at $E_{1/2} = -0.2$ V (potentials vs the ferrocene/ferrocenium redox couple), in agreement with the different electronic structures of the two bis(arene) complexes. In the case of **6**, an additional reduction event at $E_{pc} = -3.1$ V is observed that can be ascribed to a metal-centered one-electron reduction process giving an 18-electron complex.[35] The electrochemical data for the bimetallic complexes **11** and **12** suggest that the two-atom bridge exerts an electron-donating effect on the vanadium center relative to that of the single-atom bridge as the oxidation potentials of **11** ($E_{1/2} = -1.2$ V) and **12** ($E_{1/2} = -0.67$ V) are both shifted to more negative values than those of **5** and **6**, respectively (Figures S16 and S17, Supporting Information). Interestingly, the oxidation wave of the bis(benzene) derivative $[V(\eta^6\text{-}C_6H_5)_2Sn(^tBu_2)Pt(PEt_3)_2]$ (**11**) is chemically reversible, presumably a consequence of the reduced molecular strain. All these findings are consistent with previously established trends related to the electronic influence of ring substituents and *ansa* bridges for other vanadium bis(arene) systems.[14g,35,36]

In contrast, the cyclic voltammogram of polymer **13a** exhibits two distinct oxidation waves ($E_{1/2}(1) = -0.25$ V, $E_{1/2}(2) = -0.06$ V) with small peak separations of 20 and 50 mV, respectively (see Figure 4). The appearance of two successive oxidation events ($\Delta E = 0.19$ V) is strongly suggestive of some degree of electronic communication between the vanadium centers through the tin bridge. A similar redox behavior has been found for ferrocenyl polymers, such as poly(ferrocenyl)-silane or -germane.[37] In addition, spawned by the reduction processes starting around $E_{pc} = -3.0$ V, a corresponding oxidation wave at $E_{pa} = -1.8$ V is observed (see Figure S18 in

DOI: 10.1021/ja510884h
J. Am. Chem. Soc. 2015, 137, 1492−1500

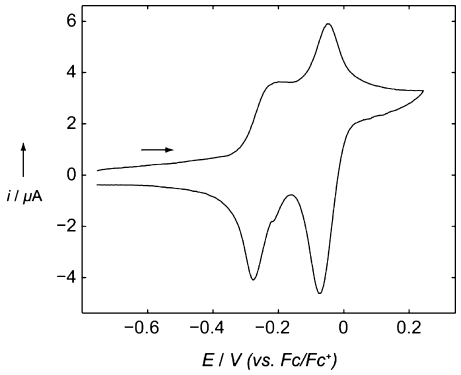

Figure 4. Cyclic voltammogram of $[V(\eta^5\text{-}C_5H_4)(\eta^7\text{-}C_7H_6)Sn^tBu_2]_n$ (**13a**) in THF/0.1 M $[n\text{-}Bu_4N][PF_6]$ at room temperature. Scan rate = 250 mV·s^{-1}.

the Supporting Information). The electrochemical behavior of **13b** parallels that of **13a**, except for the reduction events, which are missing (see Figure S19 in the Supporting Information).

Magnetic Susceptibility Measurements. The magnetic properties of the monomeric species **6** and the corresponding polymer **13b** were studied using a SQUID magnetometer at an applied magnetic field of 0.5 T in the temperature range from 295 to 2 K (Figure 5). The observed $\chi_M T$ value for **6** at room

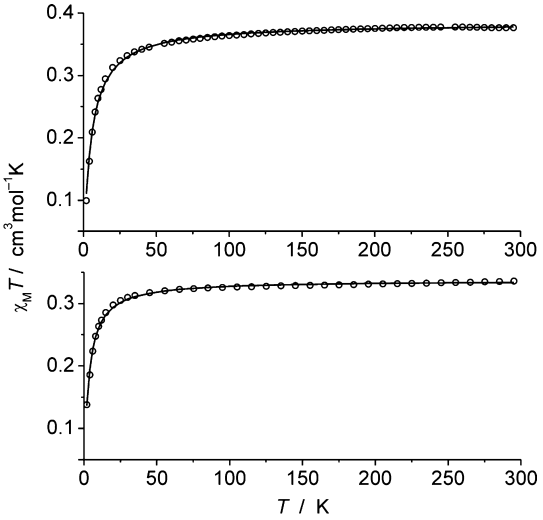

Figure 5. χ_MT vs T plot for **6** (top) and **13b** (bottom) at 5000 Oe. The solid lines represent the best fits (see text).

temperature is 0.378 cm^3·mol^{-1}·K (or 1.74 μ_B), as expected for one S = 1/2 spin carrier (0.375 cm^3·mol^{-1}·K or 1.73 μ_B for the spin-only case with g = 2.0), and stays almost constant down to 50 K. Below 50 K, $\chi_M T$ decreases to 0.100 cm^3·mol^{-1}·K, which is likely due to intermolecular antiferromagnetic spin coupling. Simulation of the experimental data (see Experimental Section) leads to best fit parameters g = 2.02 and a Weiss temperature Θ = −4.9 K, reflecting the intermolecular magnetic interactions. The Θ parameter lies in the range of −0.7 to −8.8 K found for a series of trovacenyl-based complexes.[38] Magnetic properties of **13b** are similar to those of **6**, with best fit parameters g = 1.90 and Θ = −2.9 K. Interestingly, the Θ value for mononuclear **6** is slightly larger than the Θ value for polymeric **13b**, indicating that exchange coupling through covalent bonds in **13b** should be even smaller than the intermolecular interactions through space, or of the same order of magnitude at best.

CONCLUSION

The synthesis of paramagnetic tin-containing *ansa* compounds derived from $[V(\eta^6\text{-}C_6H_6)_2]$ and $[V(\eta^5\text{-}C_5H_5)(\eta^7\text{-}C_7H_7)]$ has been reported, and their constitution has been unambiguously confirmed by elemental analysis, EI-MS, and X-ray diffraction. Because of the molecular strain present in $[V(\eta^6\text{-}C_6H_5)_2Sn^tBu_2]$ (**5**) and $[V(\eta^5\text{-}C_5H_4)(\eta^7\text{-}C_7H_6)Sn^tBu_2]$ (**6**), the bridging C−Sn bond readily oxidatively adds to bis(triethylphosphine)platinum(0), thereby indicating the possibility for metal-induced ring-opening polymerization reactions. While the bis(benzene) vanadium complex (**5**) did not show any sign of polymerization, $[V(\eta^5\text{-}C_5H_4)(\eta^7\text{-}C_7H_6)Sn^tBu_2]$ (**6**) yielded a high molecular weight polymer (M_n = 89 200 g·mol^{-1}, PDI = 1.82) using Karstedt's catalyst. The magnetic behavior as examined by SQUID indicates that the unpaired spins on the vanadium centers behave essentially independently in terms of contribution to the magnetic susceptibility of the polymer, whereas some degree of electronic metal−metal communication can be deduced from cyclic voltammetry measurements.

EXPERIMENTAL SECTION

General Considerations. All operations were performed under an atmosphere of argon by using either a glovebox or standard Schlenk line techniques. Solvents were dried by standard procedures. $[V(\eta^6\text{-}C_6H_5Li)_2]$·tmeda (**7**) (tmeda = *N*,*N*,*N*′,*N*′-tetramethylethylenediamine),[25] $[V(\eta^5\text{-}C_5H_4Li)(\eta^7\text{-}C_7H_6Li)]$·pmdta (**8**) (pmdta = *N*,*N*,*N*′,*N*′,*N*′-pentamethyldiethylenetriamine),[24c] $Cl_2Sn^tBu_2$,[39] and $[Pt(PEt_3)_3]$[40] were prepared according to published procedures. The Karstedt catalyst (2.1−2.3% w/w solution of $Pt_2[(CH_2CHSiMe_2)_2O]_3$ in xylene) was obtained commercially (ABCR). Mass spectra were recorded on a Varian 320-MS SQ mass spectrometer (EI, 70 eV), and the MALDI/TOF spectra were recorded on a Bruker Autoflex II LRF 50 in a DCTB matrix ($C_{17}H_{18}N_2$). Elemental analysis (C, H, N) was performed by combustion and gas chromatographic analysis with an Elementar Vario MICRO elemental analyzer. UV−vis spectra were recorded on a JASCO V-660 UV−vis spectrometer in an inert argon atmosphere glovebox.

Gel Permeation Chromatography. The gel permeation chromatography (GPC) experiments for polymers **13a** and **13b** were performed on an argon-flushed Agilent SECcurity GPC System (1260 Infinity) with light scattering, refractive index, and viscometer detector. The eluent was degassed and dried THF with a flow rate of 1.0 mL·min^{-1}. All molecular weights are reported relative to a monodisperse polystyrene standard. For polymer **13b** gel permeation chromatography was additionally performed on a Viscotek RImax chromatograph, equipped with an automatic sampler, a pump, an injector, and an inline degasser. The columns were contained within an oven (35 °C) and consisted of styrene/divinylbenzene gels with pore sizes ranging from 500 to 100 000 Å. THF containing 0.1% w/w $[^nBu_4N]Br$ was used as the eluent at a flow rate of 1.0 mL·min^{-1}. Samples were dissolved in the eluent (2 mg·mL^{-1}, unless otherwise stated), and toluene (1% v/v) was added to serve as a flow rate marker. These were then stirred for 1 h at room temperature and filtered with a Ministart SRP 15 filter (polytetrafluoroethylene membrane of 0.45 μm pore size) before analysis.

Dynamic Light Scattering. Dynamic light scattering (DLS) was performed on a Malvern Instruments Zetasizer Nano S using a 5 mW He-Ne laser (633 nm) at 25 °C. The correlation function was acquired in real time and analyzed with a function capable of modeling multiple exponentials. The diffusion coefficients for the component particles were then extracted. These were subsequently expressed as effective hydrodynamic radii, by volume, using the Stokes-Einstein relationship. Samples were prepared at 2 mg·mL^{-1} and filtered through a

DOI: 10.1021/ja510884h
J. Am. Chem. Soc. 2015, 137, 1492−1500

membrane filter (0.2 μm pores) into an optical glass cuvette (10.0 mm path length).

EPR Spectroscopy. CW EPR measurements at X-band (9.86 GHz) were carried out at room temperature using a Bruker ELEXSYS E580 CW EPR spectrometer. The spectral simulations were performed using MATLAB 8.0 and the EasySpin 4.5.1 toolbox.[41]

Cyclic Voltammetry. Cyclic voltammetry experiments were performed using a Gamry Instruments reference 600 potentiostat. A standard three-electrode cell configuration was employed using a platinum disk working electrode, a platinum wire counter electrode, and a silver wire, separated by a Vycor tip, serving as the reference electrode. Formal redox potentials are referenced to the ferrocene/ferrocenium redox couple ($[Cp_2Fe]^{+/0}$) either by using ferrocene or decamethylferrocene ($E_{1/2}$ = −0.427 V) as an internal standard.[42] Tetra-*n*-butylammonium hexafluorophosphate ($[n\text{-}Bu_4N][PF_6]$) was employed as the supporting electrolyte. Compensation for resistive losses (*i*R drop) was employed for all measurements.

Magnetic Measurements (SQUID). Temperature-dependent magnetic susceptibility measurements were carried out with a *Quantum-Design* MPMS-XL-5 SQUID magnetometer equipped with a 5 T magnet in the range from 295 to 2.0 K at a magnetic field of 0.5 T. The powdered sample was contained in a gelatin capsule and fixed in a nonmagnetic sample holder. Each raw data file for the measured magnetic moment was corrected for the diamagnetic contribution of the gelatin capsule according to $M^{dia}(\text{capsule}) = \chi_g \cdot m \cdot H$, with an experimentally obtained gram susceptibility of the gelatin capsule. The molar susceptibility data were corrected for the diamagnetic contribution using the Pascal constants and the increment method according to Haberditzl.[43] Experimental data were modeled by using a fitting procedure to the spin Hamiltonian for Zeeman splitting (eq 1):[44]

$$\hat{H} = g\mu_B \vec{B} \cdot \vec{S} \quad (1)$$

Temperature-independent paramagnetism (TIP) was included according to $\chi_{calc} = \chi + \text{TIP}$ (TIP = $410 \cdot 10^{-6}$ $cm^3 \cdot mol^{-1}$ for **6**). Intermolecular interactions were considered in a mean field approach by using a Weiss temperature Θ.[45] The Weiss temperature Θ (defined as $\Theta = zJS(S+1)/3k$) relates to intermolecular interactions zJ of −13.6 cm^{-1} for **6** and −8.1 cm^{-1} for **13b**, where J is the interaction parameter between two nearest-neighbor magnetic centers, k is the Boltzmann constant (0.695 $cm^{-1} \cdot K^{-1}$), and z is the number of nearest neighbors.

$[V(\eta^6\text{-}C_6H_5)_2Sn^tBu_2]$ (5). A solution of $Cl_2Sn^tBu_2$ (453 mg, 1.49 mmol) in pentane (10 mL) was added dropwise to a slurry of $[V(\eta^6\text{-}C_6H_5Li)_2]\cdot$tmeda (**7**) (500 mg, 1.49 mmol) in pentane (10 mL) at −78 °C over a period of 1 h. After complete addition, the reaction mixture was allowed to warm to ambient temperature over 2 h and was stirred for 1.5 h. The precipitated solid was then filtered off, and the red-brown filtrate was reduced to 5 mL. After storing the solution for 3 days at −70 °C, a reddish-brown solid had formed that was washed with cold pentane (3 × 5 mL) at −78 °C, and solved in pentane again, and then the unsoluble compounds were filtered off. All volatiles were removed in vacuum, and $[V(\eta^6\text{-}C_6H_5)_2Sn^tBu_2]$ (**5**) can be isolated as a yellowish-brown solid (188 mg, 0.43 mmol, 29%).

EPR (THF, 295 K): g_{iso} = 1.987, $a_{iso}(^{51}V)$ = 57.8 G; MS(EI): *m*/*z* (%) = 439 (45) $[M^+]$, 382 (12) $[M^+-(C_4H_9)]$, 325 (100) $[M^+-(C_4H_9)_2]$, 275 (36) $[Sn(C_6H_5)^{2+}]$, 247 (15) $[M^+-(C_4H_9)_2-(C_6H_5)]$, 207 (13) $[V(\eta^6\text{-}C_6H_5)_2]^{2+}$, 197 (29) $[Sn(C_6H_5)^+]$, 127 (12) $[V(C_6H_5)^+]$, 57 (100) $[C_4H_9^+]$; UV−vis (THF): λ_{max} (ε) = 325 nm (18 752 $L \cdot mol^{-1} \cdot cm^{-1}$), 436 nm (2 925 $L \cdot mol^{-1} \cdot cm^{-1}$); elemental analysis (%) calcd. for $C_{20}H_{28}SnV$ (439.07 $g \cdot mol^{-1}$): C 54.66, H 6.43; found: C 54.12, H 6.56.

$[V(\eta^5\text{-}C_5H_4)(\eta^7\text{-}C_7H_6)Sn^tBu_2]$ (6). A slurry of $[V(\eta^5\text{-}C_5H_4Li)(\eta^7\text{-}C_7H_6Li)]\cdot$pmdta (**8**) (600 mg, 1.53 mmol) in pentane (20 mL) was treated dropwise with a solution of $Cl_2Sn^tBu_2$ (488 mg, 1.61 mmol) in pentane (20 mL) at −78 °C over a period of 1 h. The purple reaction mixture was allowed to warm to ambient temperature during 3.5 h and stirred for 2.5 h. All volatiles were removed under vacuum, and the residue was extracted in pentane. The solution was concentrated to 5 mL and stored at −70 °C for 3 days. The resulting purple solid was washed with cold pentane (3 × 10 mL) at −78 °C, solved in pentane, and filtered off. All volatiles were removed in vacuum to afford $[V(\eta^5\text{-}C_5H_4)(\eta^7\text{-}C_7H_6)Sn^tBu_2]$ (**6**) as a purple solid (256 mg, 0.58 mmol, 38%).

EPR (THF, 295 K): g_{iso} = 1.984, $a_{iso}(^{51}V)$ = 68.3 G; MS(EI) *m*/*z* (%) = 439 (2) $[M^+]$, 325 (8) $[M^+-(C_4H_9)_2]$, 247 (5) $[M^+-(C_4H_9)-(C_7H_6)-(CH_3)_3]$, 207 (13) $[V(\eta^5\text{-}C_5H_4)(\eta^7\text{-}C_7H_6)^{2+}]$, 178 (5) $[Sn(C_4H_{10})^+]$, 116 (7) $[V(\eta^5\text{-}C_5H_4)]^+$, 57 (100) $[(C_4H_9)^+]$; MALDI/TOF *m*/*z*: 689 $[M^+\cdot C_{17}H_{18}N_2]$; UV−vis (THF): λ_{max} (ε) = 213 nm (47 075 $L \cdot mol^{-1} \cdot cm^{-1}$), 320 nm (sh), 611 nm (64 $L \cdot mol^{-1} \cdot cm^{-1}$); elemental analysis (%) calcd. for $C_{20}H_{28}SnV$ (439.07 $g \cdot mol^{-1}$): C 54.66, H 6.43; found: C 54.85, H 6.47.

$[V(\eta^6\text{-}C_6H_5)_2Sn^tBu_2Pt(PEt_3)_2]$ (11). A mixture of $[V(\eta^6\text{-}C_6H_5)_2Sn^tBu_2]$ (**5**) (50 mg, 0.11 mmol) and $[Pt(PEt_3)_3]$ (63 mg, 0.11 mmol) in benzene (5 mL) was heated at 60 °C over a period of 24 h. The red-brown solution was then filtrated over a short pad of Celite, and all volatiles were removed under vacuum. The resulting residue was washed with cold pentane (3 × 5 mL) at −78 °C and vacuum-dried to yield $[V(\eta^6\text{-}C_6H_5)_2Sn^tBu_2Pt(PEt_3)_2]$ (**11**) as a red-brown solid (47 mg, 0.05 mmol, 47%).

EPR (THF, 295 K): g_{iso} = 1.993, $a_{iso}(^{51}V)$ = 62.3 G; UV−vis (THF): λ_{max} (ε) = 341 nm (17 692 $L \cdot mol^{-1} \cdot cm^{-1}$), 462 nm (3 157 $L \cdot mol^{-1} \cdot cm^{-1}$); elemental analysis (%) calcd. for $C_{32}H_{58}P_2PtSnV$ (870.21 $g \cdot mol^{-1}$): C 44.12, H 6.72; found: C 44.02, H 6.72.

$[V(\eta^5\text{-}C_5H_4)(\eta_7\text{-}C_7H_6)Sn^tBu_2Pt(PEt_3)_2]$ (12). A solution of $[V(\eta^5\text{-}C_5H_4)(\eta^7\text{-}C_7H_6)Sn^tBu_2]$ (**6**) (50 mg, 0.11 mmol) and $[Pt(PEt_3)_3]$ (63 mg, 0.11 mmol) in benzene (5 mL) was heated at 60 °C over a period of 72 h. All volatiles were removed from the greenish solution, and the gray solid was washed with hexane (3 × 5 mL). The residue was solved in toluene (10 mL) and filtrated, and the solvent was removed under high vacuum to afford $[V(\eta^5\text{-}C_5H_4)(\eta^7\text{-}C_7H_6)Sn^tBu_2Pt(PEt_3)_2]$ (**12**) as a gray solid (39 mg, 0.05 mmol, 39%).

EPR (THF, 295 K): g_{iso} = 1.988, $a_{iso}(^{51}V)$ = 71.1 G; UV−vis (THF): λ_{max} (ε) = 216 nm (39 118 $L \cdot mol^{-1} \cdot cm^{-1}$), 290 nm (sh), 350 nm(sh), 571 nm (104 $L \cdot mol^{-1} \cdot cm^{-1}$); elemental analysis (%) calcd. for $C_{32}H_{58}P_2PtSnV$ (870.21 $g \cdot mol^{-1}$): C 44.12, H 6.72; found: C 44.54, H 6.73.

Polymerization of $[V(\eta^5\text{-}C_5H_4)(\eta^7\text{-}C_7H_6)Sn^tBu_2]$ (6). A greaseless Schlenk flask was equipped with a solution of $[V(\eta^5\text{-}C_5H_4)(\eta^7\text{-}C_7H_6)Sn^tBu_2]$ (**6**) (**13a**, 100 mg, 0.23 mmol; **13b**, 50 mg, 0.12 mmol) in toluene (2 mL) and the Karstedt catalyst (**13a**, 0.35 mL, 3.0 mol % Pt; **13b**, 0.14 mL, 2.5 mol % Pt), and the color changed immediately from purple to dark green. The mixture was heated to 60 °C for 24 h and then precipitated into rapidly stirred hexane. The resulting solid was dissolved in toluene, and the precipitation was repeated twice to afford $[V(\eta^5\text{-}C_5H_4)(\eta^7\text{-}C_7H_6)Sn^tBu_2]_n$ (**13a** and **13b**) as a light (**13a**) or dark (**13b**) purple solid, which was dried in vacuum (**13a**, 46 mg, 46%; **13b**, 22 mg, 44%).

13a: EPR (THF, 295 K): g_{iso} = 1.974; UV−vis (THF): λ_{max} = 269 nm (maxima), 284 nm (maxima), 310 nm (sh), 456 nm (sh), 582 nm (maxima); GPC (in THF versus polystyrene): M_w = 35 155 $g \cdot mol^{-1}$, M_n = 19 294 $g \cdot mol^{-1}$, M_w/M_n = 1.82.

13b: UV−vis (THF): λ_{max} = 258 nm (maxima), 310 nm (sh), 370 nm (sh), 467 nm (maxima), 602 nm (maxima); GPC (in THF versus polystyrene): M_w = 103 666 $g \cdot mol^{-1}$, M_n = 43 222 $g \cdot mol^{-1}$, M_w/M_n = 2.40; GPC (in THF containing 0.1% w/w $[^nBu_4N]Br$): M_w = 162 400 $g \cdot mol^{-1}$, M_n = 89 200 $g \cdot mol^{-1}$, M_w/M_n = 1.82; DLS: R_h = 3.8 nm (62.8%), 14.5 nm (37.2%).

Single-Crystal X-ray Structure Determination. The crystal data of **5** and **11** were collected on a Bruker X8APEX diffractometer with a charge-coupled device (CCD) area detector and multilayer mirror monochromated $Mo_{K\alpha}$ radiation. The crystal data of **6** and **12** were collected on a Bruker APEX diffractometer with a CCD area detector and graphite monochromated $Mo_{K\alpha}$ radiation. The structures were solved using direct methods, refined with the Shelx software package,[46] and expanded using Fourier techniques. All non-hydrogen atoms were refined anisotropically. Hydrogen atoms were included in structure factor calculations. All hydrogen atoms were assigned to idealized geometric positions.

DOI: 10.1021/ja510884h
J. Am. Chem. Soc. 2015, 137, 1492−1500

Crystallographic data have been deposited with the Cambridge Crystallographic Data Center as supplementary publication no. CCDC-1029707 (**5**), CCDC-1029708 (**6**), CCDC-1029709 (**11**) and CCDC-1029710 (**12**). These data can be obtained free of charge from The Cambridge Crystallographic Data Centre via www.ccdc.cam.ac.uk/data_request/cif.

Crystal data for **5**: $C_{20}H_{28}SnV$, M_r = 438.05, orange block, 0.24 × 0.12 × 0.04 mm^3, monoclinic space group $C2/c$, a = 12.5094(12) Å, b = 9.8617(9) Å, c = 15.3826(15) Å, β = 107.849(4)°, V = 1806.3(3) Å^3, Z = 4, ρ_{calcd} = 1.611 g·cm^{-3}, μ = 1.895 mm^{-1}, $F(000)$ = 884, T = 108(2) K, R_1 = 0.0124, wR^2 = 0.0313, 2216 independent reflections [$2\theta \leq 56.64°$] and 104 parameters.

Crystal data for **6**: $C_{20}H_{28}SnV$, M_r = 438.05, violet block, 0.18 × 0.14 × 0.05 mm^3, monoclinic space group $P2_1/c$, a = 12.8987(16) Å, b = 9.3160(12) Å, c = 16.749(2) Å, β = 110.477(2)°, V = 1885.4(4) Å^3, Z = 4, ρ_{calcd} = 1.543 g·cm^{-3}, μ = 1.816 mm^{-1}, $F(000)$ = 884, T = 173(2) K, R_1 = 0.0365, wR^2 = 0.0782, 3682 independent reflections [$2\theta \leq 52.16°$] and 205 parameters.

Crystal data for **11**: $C_{32}H_{58}P_2PtSnV$, M_r = 869.44, orange block, 0.178 × 0.099 × 0.047 mm^3, monoclinic space group $P2_1/c$, a = 21.9178(14) Å, b = 18.6844(11) Å, c = 17.9740(11) Å, β = 109.179(3)°, V = 6952.2(7) Å^3, Z = 8, ρ_{calcd} = 1.661 g·cm^{-3}, μ = 5.102 mm^{-1}, $F(000)$ = 3448, T = 100(2) K, R_1 = 0.0709, wR^2 = 0.0965, 13 538 independent reflections [$2\theta \leq 52.08°$] and 691 parameters.

Crystal data for **12**: $C_{32}H_{58}P_2PtSnV$, M_r = 869.44, colorless plate, 0.24 × 0.19 × 0.03 mm^3, monoclinic space group $P2_1/n$, a = 11.812(2) Å, b = 19.413(4) Å, c = 16.299(3) Å, β = 102.23(3)°, V = 3652.7(13) Å^3, Z = 5, ρ_{calcd} = 1.976 g·cm^{-3}, μ = 6.069 mm^{-1}, $F(000)$ = 2155, T = 173(2) K, R_1 = 0.0660, wR^2 = 0.1271, 7153 independent reflections [$2\theta \leq 52.04°$] and 346 parameters.

■ ASSOCIATED CONTENT

Supporting Information

EPR, GPC, DLS, cyclic voltammetry, and UV−vis data of all species. This material is available free of charge via the Internet at http://pubs.acs.org.

■ AUTHOR INFORMATION

Corresponding Author

* h.braunschweig@uni-wuerzburg.de

Notes

The authors declare no competing financial interest.

■ ACKNOWLEDGMENTS

This work was gratefully supported by the Deutsche Forschungsgemeinschaft (DFG). We also thank Prof. Ian Manners for assistance with polymer characterization.

■ REFERENCES

(1) Withers, H. P., Jr.; Seyferth, D. *Organometallics* **1982**, *1*, 1283.

(2) Brandt, P. F.; Rauchfuss, T. B. *J. Am. Chem. Soc.* **1992**, *114*, 1926.

(3) (a) Heilmann, J. B.; Qin, Y.; Jaekle, F.; Lerner, H.-W.; Wagner, M. *Inorg. Chim. Acta* **2006**, *359*, 4802. (b) Heilmann, J. B.; Scheibitz, M.; Qin, Y.; Sundararaman, A.; Jaekle, F.; Kretz, T.; Bolte, M.; Lerner, H.-W.; Holthausen, M. C.; Wagner, M. *Angew. Chem.* **2006**, *118*, 934; *Angew. Chem., Int. Ed.* **2006**, *45*, 920. (c) Scheibitz, M.; Li, H.; Schnorr, J.; Sánchez Perucha, A.; Bolte, M.; Lerner, H.-W.; Jaekle, F.; Wagner, M. *J. Am. Chem. Soc.* **2009**, *131*, 16319. (d) Cui, C.; Heilmann-Brohl, J.; Sánchez Perucha, A.; Thomson, M. D.; Roskos, H. G.; Wagner, M.; Jaekle, F. *Macromolecules* **2010**, *43*, 5256.

(4) (a) Foucher, D. A.; Tang, B.-Z.; Manners, I. *J. Am. Chem. Soc.* **1992**, *114*, 6246. (b) Finckh, W.; Tang, B.-Z.; Foucher, D. A.; Zamble, D. B.; Ziembinski, R.; Lough, A. J.; Manners, I. *Organometallics* **1993**, *12*, 823.

(5) (a) Abd-El-Aziz, A. S.; Manners, I. *Frontiers in Transition Metal Containing Polymers*; John Wiley and Sons: Hoboken, NJ, 2007. (b) Bellas, V.; Rehahn, M. *Angew. Chem.* **2007**, *119*, 5174; *Angew. Chem., Int. Ed.* **2007**, *46*, 5082. (c) Herbert, D. E.; Mayer, U. F. J.; Manners, I. *Angew. Chem.* **2007**, *119*, 5152; *Angew. Chem., Int. Ed.* **2007**, *46*, 5060.

(6) (a) Berenbaum, A.; Braunschweig, H.; Dirk, R.; Englert, U.; Green, J. C.; Jaekle, F.; Lough, A. J.; Manners, I. *J. Am. Chem. Soc.* **2000**, *122*, 5765. (b) Schachner, J. A.; Lund, C. L.; Quail, J. W.; Mueller, J. *Organometallics* **2005**, *24*, 785. (c) Schachner, J. A.; Lund, C. L.; Quail, J. W.; Mueller, J. *Organometallics* **2005**, *24*, 4483. (d) Bagh, B.; Sadeh, S.; Green, J. C.; Mueller, J. *Chem.—Eur. J.* **2014**, *20*, 2318.

(7) (a) Stoeckli-Evans, H.; Osborne, A. G.; Whiteley, R. H. *J. Organomet. Chem.* **1980**, *194*, 91. (b) Foucher, D. A.; Edwards, M.; Burrow, R. A.; Lough, A. J.; Manners, I. *Organometallics* **1994**, *13*, 4959. (c) Rulkens, R.; Lough, A. J.; Manners, I. *Angew. Chem.* **1996**, *108*, 1929; *Angew. Chem., Int. Ed.* **1996**, *35*, 1805. (d) Jäkle, F.; Rulkens, R.; Zech, G.; Foucher, D. A.; Lough, A. J.; Manners, I. *Chem.—Eur. J.* **1998**, *4*, 2117.

(8) (a) Seyferth, D.; Withers, H. P. *Organometallics* **1982**, *1*, 1275. (b) Butler, I. R.; Cullen, W. R.; Einstein, F. W. B.; Rettig, S. J.; Willis, A. J. *Organometallics* **1983**, *2*, 128.

(9) (a) Pudelski, J. K.; Gates, D. P.; Rulkens, R.; Lough, A. J.; Manners, I. *Angew. Chem.* **1995**, *107*, 1633; *Angew. Chem., Int. Ed.* **1995**, *34*, 1506. (b) Rulkens, R.; Gates, D. P.; Balaishis, D.; Pudelski, J. K.; Mcintosh, D. F.; Lough, A. J.; Manners, I. *J. Am. Chem. Soc.* **1997**, *119*, 10976.

(10) Broussier, R.; Da Rold, A.; Gautheron, B.; Dromzee, Y.; Jeannin, Y. *Inorg. Chem.* **1990**, *29*, 1817.

(11) (a) Whittell, G. R.; Partridge, B. M.; Presley, O. C.; Adams, C. J.; Manners, I. *Angew. Chem.* **2008**, *120*, 4426; *Angew. Chem., Int. Ed.* **2008**, *47*, 4354. (b) Matas, I.; Whittell, G. R.; Partridge, B. M.; Holland, J. P.; Haddow, M. F.; Green, J. C.; Manners, I. *J. Am. Chem. Soc.* **2010**, *132*, 13279.

(12) (a) Mammano, N. J.; Zalkin, A.; Landers, A.; Rheingold, A. L. *Inorg. Chem.* **1977**, *16*, 297. (b) Miller, J. S.; Calabrese, J. C.; Rommelmann, H.; Chittipeddi, S. R.; Zhang, J. H.; Reiff, W. M.; Epstein, A. J. *J. Am. Chem. Soc.* **1987**, *109*, 769. (c) Webb, R. J.; Lowery, M. D.; Shiomi, Y.; Sorai, M.; Wittebort, R. J.; Hendrickson, D. N. *Inorg. Chem.* **1992**, *31*, 5211. (d) O'Connor, A. R.; Nataro, C.; Golen, J. A.; Rheingold, A. L. *J. Organomet. Chem.* **2004**, *689*, 2411. (e) Drewitt, M. J.; Barlow, S.; O'Hare, D.; Nelson, J. M.; Nguyen, P.; Manners, I. *Chem. Commun.* **1996**, 2153. (f) Watanabe, M.; Sato, K.; Motoyama, I.; Sano, H. *Chem. Lett.* **1983**, 1775. (g) Masson, G.; Herbert, D. E.; Whittell, G. R.; Holland, J. P.; Lough, A. J.; Green, J. C.; Manners, I. *Angew. Chem.* **2009**, *121*, 5061; *Angew. Chem., Int. Ed.* **2009**, *48*, 4961.

(13) (a) Walczak, M.; Walczak, K.; Mink, R.; Rausch, M. D.; Stucky, G. *J. Am. Chem. Soc.* **1978**, *100*, 6382. (b) Butler, I. R.; Cullen, W. R.; Ni, J.; Rettig, S. J. *Organometallics* **1985**, *4*, 2196. (c) Rausch, M. D.; Ciappenelli, D. J. *J. Organomet. Chem.* **1967**, *10*, 127.

(14) (a) Seyferth, D. *Organometallics* **2002**, *21*, 1520. (b) Braunschweig, H.; Kupfer, T. *Organometallics* **2007**, *26*, 4634. (c) Hevia, E.; Honeyman, G. W.; Kennedy, A. R.; Mulvey, R. E.; Sherrington, D. C. *Angew. Chem.* **2005**, *117*, 70; *Angew. Chem., Int. Ed.* **2005**, *44*, 68. (d) Green, M. L. H.; Treurnicht, I.; Bandy, J. A.; Gourdon, A.; Prout, K. *J. Organomet. Chem.* **1986**, *306*, 145. (e) Braunschweig, H.; Buggisch, N.; Englert, U.; Homberger, M.; Kupfer, T.; Leusser, D.; Lutz, M.; Radacki, K. *J. Am. Chem. Soc.* **2007**, *129*, 4840. (f) Lund, C. L.; Schachner, J. A.; Quail, J. W.; Mueller, J. *J. Am. Chem. Soc.* **2007**, *129*, 9313. (g) Elschenbroich, C.; Hurley, J.; Metz, B.; Massa, W.; Baum, G. *Organometallics* **1990**, *9*, 889.

(15) (a) Ogasa, M.; Rausch, M. D.; Rogers, R. D. *J. Organomet. Chem.* **1991**, *403*, 279. (b) Tamm, M.; Kunst, A.; Bannenberg, T.; Herdtweck, E.; Sirsch, P.; Elsevier, C. J.; Ernsting, J. M. *Angew. Chem.* **2004**, *116*, 5646; *Angew. Chem., Int. Ed.* **2004**, *43*, 5530. (c) Tamm, M.; Kunst, A.; Bannenberg, T.; Randoll, S.; Jones, P. G. *Organometallics* **2007**, *26*, 417. (d) Braunschweig, H.; Fuß, M.; Mohapatra, S. K.; Kraft, K.; Kupfer, T.; Lang, M.; Radacki, K.; Daniliuc, C. G.; Jones, P. G.; Tamm, M. *Chem.—Eur. J.* **2010**, *16*, 11732. (e) Tagne Kuate, A. C.; Daniliuc, C. G.; Jones, P. G.; Tamm,

DOI: 10.1021/ja510884h
J. Am. Chem. Soc. 2015, 137, 1492−1500

M. *Eur. J. Inorg. Chem.* **2012**, 1727. (f) Fischer, E. O.; Breitschaft, S. *Chem. Ber.* **1966**, *99*, 2905. (g) Braunschweig, H.; Lutz, M.; Radacki, K. *Angew. Chem.* **2005**, *117*, 5792; *Angew. Chem., Int. Ed.* **2005**, *44*, 5647. (h) Bartole-Scott, A.; Braunschweig, H.; Kupfer, T.; Lutz, M.; Manners, I.; Nguyen, T.-L.; Radacki, K.; Seeler, F. *Chem.—Eur. J.* **2006**, *12*, 1266.

(16) Berenbaum, A.; Manners, I. *Dalton Trans.* **2004**, 2057.

(17) (a) Anderson, J. E.; Maher, E. T.; Kool, L. B. *Organometallics* **1991**, *10*, 1248. (b) Evans, S.; Green, J. C.; Jackson, S. E.; Higginson, B. *J. Chem. Soc., Dalton Trans.* **1974**, 304.

(18) (a) Benn, R.; Blank, N. E.; Haenel, M. W.; Klein, J.; Koray, A. R.; Weidenhammer, K.; Ziegler, M. L. *Angew. Chem.* **1980**, *92*, 45; *Angew. Chem., Int. Ed.* **1980**, *19*, 44. (b) Shapiro, P. J.; Sinnema, P.-J.; Perrotin, P.; Budzelaar, P. H. M.; Weihe, H.; Twamley, B.; Zehnder, R. A.; Nairn, J. J. *Chem.—Eur. J.* **2007**, *13*, 6212.

(19) Jeffrey, J.; Mawby, R. J.; Hursthouse, M. B.; Walker, N. P. C. *J. Chem. Soc., Chem. Commun.* **1982**, 1411.

(20) (a) Mayer, U. F. J.; Gilroy, J. B.; O'Hare, D.; Manners, I. *J. Am. Chem. Soc.* **2009**, *131*, 10382. (b) Mayer, U. F. J.; Charmant, J. P. H.; Rae, J.; Manners, I. *Organometallics* **2008**, *27*, 1524. (c) Fox, S.; Dunne, J. P.; Tacke, M.; Schmitz, D.; Dronskowski, R. *Eur. J. Inorg. Chem.* **2002**, 3039.

(21) Braunschweig, H.; Fuss, M.; Kupfer, T.; Radacki, K. *J. Am. Chem. Soc.* **2011**, *133*, 5780.

(22) Baljak, S.; Russell, A. D.; Binding, S. C.; Haddow, M. F.; O'Hare, D.; Manners, I. *J. Am. Chem. Soc.* **2014**, *136*, 5864.

(23) (a) Elschenbroich, C.; Gerson, F. *Chimia* **1974**, *28*, 720. (b) Elschenbroich, C.; Schmidt, E.; Metz, B.; Harms, K. *Organometallics* **1995**, *14*, 4043. (c) Braunschweig, H.; Kaupp, M.; Adams, C. J.; Kupfer, T.; Radacki, K.; Schinzel, S. *J. Am. Chem. Soc.* **2008**, *130*, 11376.

(24) (a) Elschenbroich, C.; Paganelli, F.; Nowotny, M.; Neumueller, B.; Burghaus, O. *Z. Anorg. Allg. Chem.* **2004**, *630*, 1599. (b) Braunschweig, H.; Lutz, M.; Radacki, K.; Schaumloeffel, A.; Seeler, F.; Unkelbach, C. *Organometallics* **2006**, *25*, 4433. (c) Adams, C. J.; Braunschweig, H.; Fuß, M.; Kraft, K.; Kupfer, T.; Manners, I.; Radacki, K.; Whittell, G. R. *Chem.—Eur. J.* **2011**, *17*, 10379.

(25) Braunschweig, H.; Adams, C. J.; Kupfer, T.; Manners, I.; Richardson, R. M.; Whittell, G. R. *Angew. Chem.* **2008**, *120*, 3886; *Angew. Chem., Int. Ed.* **2008**, *47*, 3826.

(26) (a) Elschenbroich, C.; Bretschneider-Hurley, A.; Hurley, J.; Massa, W.; Wocadlo, S.; Pebler, J. *Inorg. Chem.* **1993**, *32*, 5421. (b) Elschenbroich, C.; Bretschneider-Hurley, A.; Hurley, J.; Behrendt, A.; Massa, W.; Wocadlo, S.; Reijerse, E. *Inorg. Chem.* **1995**, *34*, 743.

(27) (a) Elschenbroich, C.; Lu, F.; Nowotny, M.; Burghaus, O.; Pietzonka, C.; Harms, K. *Organometallics* **2007**, *26*, 4025. (b) Elschenbroich, C.; Lu, F.; Burghaus, O.; Pietzonka, C.; Harms, K. *Chem. Commun.* **2007**, 3201.

(28) Braunschweig, H.; Breher, F.; Capper, S.; Dueck, K.; Fuß, M.; Jimenez-Halla, J. O. C.; Krummenacher, I.; Kupfer, T.; Nied, D.; Radacki, K. *Chem.—Eur. J.* **2013**, *19*, 270.

(29) Rulkens, R.; Lough, A. J.; Manners, I.; Lovelace, S. R.; Grant, C.; Geiger, W. E. *J. Am. Chem. Soc.* **1996**, *118*, 12683.

(30) Tamm, M.; Kunst, A.; Herdtweck, E. *Chem. Commun.* **2005**, 1729.

(31) Fetters, L.; Hadjichristidis, N.; Lindner, J.; Mays, J. *J. Phys. Chem. Ref. Data* **1994**, *23*, 619.

(32) Simulations were performed with *EasySpin*: Stoll, S.; Schweiger, A. *J. Magn. Reson.* **2006**, *178*, 42.

(33) Andrews, M. P.; Mattar, S. M.; Ozin, G. A. *J. Phys. Chem.* **1986**, *90*, 1037.

(34) (a) Green, J. C.; Ketkov, S. Y. *Organometallics* **1996**, *15*, 4747. (b) Gulick, W. M.; Geskei, D. H. *Inorg. Chem.* **1967**, *6*, 1320.

(35) Elschenbroich, C.; Bilger, E.; Metz, B. *Organometallics* **1991**, *10*, 2823.

(36) Elschenbroich, C.; Schmidt, E.; Gondrum, R.; Metz, B.; Burghaus, O.; Massa, W.; Wocadlo, S. *Organometallics* **1997**, *16*, 4589.

(37) Foucher, D. A.; Honeyman, C. H.; Nelson, J. M.; Tang, B. Z.; Manners, I. *Angew. Chem.* **1993**, *105*, 1843; *Angew. Chem., Int. Ed.* **1993**, *32*, 1709.

(38) Elschenbroich, C.; Plackmeyer, J.; Nowotny, M.; Behrendt, A.; Harms, K.; Pebler, J.; Burghaus, O. *Chem.—Eur. J.* **2005**, *11*, 7427.

(39) Englich, U.; Hermann, U.; Prass, I.; Schollmeier, T.; Ruhlandt-Senge, K.; Uhlig, F. *J. Organomet. Chem.* **2002**, *646*, 271.

(40) (a) Yoshida, T.; Matsuda, T.; Otsuka, S.; Parshall, G. W.; Peet, W. G. *Inorg. Synth.* **1979**, *19*, 110. (b) Yoshida, T.; Matsuda, T.; Otsuka, S.; Parshall, G. W.; Peet, W. G.; Binger, P.; Brinkmann, A.; Wedemann, P. *Inorg. Synth.* **1979**, *19*, 107.

(41) Stoll, S.; Schweiger, A. *J. Magn. Reson.* **2006**, *178*, 42.

(42) Noviandri, I.; Brown, K. N.; Fleming, D. S.; Gulyas, P. T.; Lay, P. A.; Masters, A. F.; Phillips, L. *J. Phys. Chem. B* **1999**, *103*, 6713.

(43) (a) Haberditzel, W. *Angew. Chem.* **1966**, *78*, 277; *Angew. Chem., Int. Ed. Engl.* **1966**, *5*, 288. (b) Bain, G. A.; Berry, J. F. *J. Chem. Educ.* **2008**, *85*, 532.

(44) Simulation of the experimental magnetic data was performed with the *julX* program (Bill, E. Max-Planck Institute for Chemical Energy Conversion: Mülheim/Ruhr, Germany).

(45) Kahn, O. *Molecular Magnetism*; VCH: Weinheim, Germany, 1993.

(46) Sheldrick, G. *Acta Crystallogr.* **2008**, *A64*, 112.

DOI: 10.1021/ja510884h
J. Am. Chem. Soc. 2015, 137, 1492−1500